A PARAFAC-BASED TECHNIQUE FOR DETECTION AND LOCALIZATION OF MULTIPLE TARGETS IN A MIMO RADAR SYSTEM

Dimitri Nion and Nicholas D. Sidiropoulos

Dept. of Electronic and Computer Engineering, Technical University of Crete, 73100 Chania, Greece.
E-mails: {nion, nikos}@telecom.tuc.gr

ABSTRACT

In this paper, we show that the problem of detection and localization of multiple targets in a bistatic MIMO radar system can be solved by Parallel Factor (PARAFAC) analysis. Our method is deterministic and fully capitalizes on the strong algebraic structure of the received data, where the Radar Cross Section (RCS) fluctuation is not regarded as a nuisance parameter but rather as a source of time diversity. Simulation results show that our technique outperforms existing beamforming-based radar imaging methods at a lower complexity.

Index Terms— MIMO radars, PARAFAC, DOA-DOD estimation

1. INTRODUCTION

Recently, the concept of Multiple-Input Multiple-Output (MIMO) radar has drawn considerable attention (see [1], [2] and references therein). A MIMO radar utilizes multiple antennas at both the transmitter and receiver, but unlike conventional phased-array radars, it can transmit linearly independent waveforms. This waveform diversity endows MIMO radars with superior capabilities relative to phased-array radars. One can distinguish two main classes of MIMO radars: MIMO radars with widely separated antennas [2] and MIMO radars with colocated antennas [1]. The first class capitalizes on the rich scattering properties of a target and mitigates Radar Cross Section (RCS) fluctuations by transmitting linearly independent signals from sufficiently spaced antennas that illuminate the target from ideally decorrelated aspects. The second class allows to model a target as a point-source in the far-field and capitalizes on the MIMO spatial signatures to estimate the parameters of interest via coherent processing.

In this paper, we focus on the problems of detection and estimation of Direction Of Arrival (DOA) and Direction Of Departure (DOD) of multiple targets present in the same

range-bin for a bistatic MIMO radar system where the transmit and receive arrays have colocated antennas. In [3], the monostatic case is considered, i.e., each target has the same localization w.r.t. both arrays. It is shown that, for a given pulse period, the angles can be found via a beamforming-based one-dimensional imaging method. However, changing a target aspect by as little as one milliradian may result in variations of the reflected power of 20 dB or more, which translates to a target scintillation phenomenon caused by fading. Consequently, if the reflection coefficients of the targets vary from pulse to pulse (Swerling II model), application of the radar-imaging technique [3] on a per-pulse basis does not allow detection and accurate localization of all targets for every pulse. In [4], the data model of [3] is extended to the bistatic case and considers several pulse periods through a Swerling II target RCS model. The method proposed in [4] for DOA and DOD estimation is a two-dimensional (2-D) radar imaging method, which consists of looking for the peaks of a 2-D Capon beamformer output, the latter being computed for every pair of angles in a region of interest.

Starting from the same data-model as [4], we show that the detection and localization of multiple targets can alternatively be achieved by Parallel Factor (PARAFAC) analysis. Our PARAFAC-based technique is deterministic and fully exploits the algebraic structure of the received data, where the RCS fluctuations are not regarded as a nuisance parameter but rather as a source of time diversity. As we will illustrate by simulation results, our method outperforms 2-D Capon at a lower complexity.

Notation. $\mathbf{Y}^T$ is the transpose of $\mathbf{Y}$ and $\mathbf{Y}^H$ its complex conjugate transpose. $\text{vec}(\mathbf{Y})$ is the operator that stacks the columns of $\mathbf{Y}$ one after each other in a single vector. $\text{diag}(\mathbf{y})$ is a diagonal matrix that holds the entries of $\mathbf{y}$ on its diagonal. The $P \times P$ identity matrix is denoted by $\mathbf{I}_P$. The Khatri-Rao product is denoted $\odot$, i.e., $[\mathbf{a}_1, \ldots, \mathbf{a}_I] \odot [\mathbf{b}_1, \ldots, \mathbf{b}_I] = [\mathbf{a}_1 \otimes \mathbf{b}_1, \ldots, \mathbf{a}_I \otimes \mathbf{b}_I]$, where $\otimes$ is the Kronecker product.

2. PROBLEM STATEMENT

Let us consider a MIMO radar system with the following parameters:
- a transmit array of M_t colocated antennas,

- a receive array of M_r colocated antennas,
- K targets in a particular range-bin of interest,
- $\mathbf{S} \in \mathbb{C}^{M_t \times N}$ holds M_t mutually orthogonal transmitted pulse waveforms, N being the number of samples per pulse period,
- $\{\theta_{t_k}\}_{k=1}^K$, $\{\theta_{r_k}\}_{k=1}^K$ are the locations of the targets w.r.t. transmit and receive arrays, respectively,
- $\mathbf{A}(\theta_t) = [\mathbf{a}(\theta_{t_1}), \ldots, \mathbf{a}(\theta_{t_K})]$ is the $M_t \times K$ transmit steering matrix and $\mathbf{B}(\theta_r) = [\mathbf{b}(\theta_{r_1}), \ldots, \mathbf{b}(\theta_{r_K})]$ the $M_r \times K$ receive steering matrix,
- Q transmitted pulses,
- β_{kq} is the reflection coefficient of the kth target during the qth pulse.

Furthermore, we assume that the range of any target is much larger than the aperture of the transmit and receive arrays. A target is modeled as a point-source in the far-field, which is commonly assumed in conventional radar systems, as well as in MIMO radar systems with colocated antennas [1]. The steering matrices $\mathbf{B}(\theta_r)$ and $\mathbf{A}(\theta_t)$ are assumed constant over the duration of the Q pulses, while the target reflection coefficients are varying independently from pulse to pulse (Swerling II model). Assuming non-dispersive propagation, the received signal can be written as [4]

$$\mathbf{X}_q = \mathbf{B}(\theta_r)\mathbf{\Sigma}_q\mathbf{A}^T(\theta_t)\mathbf{S} + \mathbf{W}_q, \quad q = 1, \ldots, Q, \quad (1)$$

where $\mathbf{X}_q \in \mathbb{C}^{M_r \times N}$ collects the N samples received by each antenna for the qth pulse period, $\mathbf{\Sigma}_q = \text{diag}(\mathbf{c}_q)$, $\mathbf{c}_q = [\beta_{1q}, \ldots, \beta_{Kq}]$, and $\mathbf{W}_q \in \mathbb{C}^{M_r \times N}$ is the interference and noise term.

If we right-multiply both sides of (1) by $\frac{1}{N}\mathbf{S}^H$, the resulting model after this matched-filtering operation is

$$\mathbf{Y}_q = \mathbf{B}(\theta_r)\mathbf{\Sigma}_q\mathbf{A}^T(\theta_t) + \mathbf{Z}_q, \quad q = 1, \ldots, Q, \quad (2)$$

where

$$\mathbf{Y}_q = \frac{1}{N}\mathbf{X}_q\mathbf{S}^H, \quad \mathbf{Z}_q = \frac{1}{N}\mathbf{W}_q\mathbf{S}^H. \quad (3)$$

Let us now vectorize (2):

$$\mathbf{y}_q = (\mathbf{A}(\theta_t) \odot \mathbf{B}(\theta_r))\mathbf{c}_q^T + \mathbf{z}_q, \quad q = 1, \ldots, Q, \quad (4)$$

where $\mathbf{y}_q = \text{vec}(\mathbf{Y}_q)$, $\mathbf{z}_q = \text{vec}(\mathbf{Z}_q)$.

Considering the Q pulses, (4) can be written in the following compact form

$$\mathbf{Y} = (\mathbf{A}(\theta_t) \odot \mathbf{B}(\theta_r))\mathbf{C}^T + \mathbf{Z}, \quad (5)$$

where $\mathbf{Y} = [\mathbf{y}_1, \ldots, \mathbf{y}_Q]$ and $\mathbf{Z} = [\mathbf{z}_1, \ldots, \mathbf{z}_Q]$ are of size $M_t M_r \times Q$ and $\mathbf{C}^T = [\mathbf{c}_1^T, \ldots, \mathbf{c}_Q^T]$ is of size $K \times Q$. The model (5) was established in [4] and can be considered as the generalization of the single-pulse multi-target model [3] to the multi-pulse Swerling II multi-target model. Given (5), the following Capon estimator of (θ_t, θ_r) was derived in [4]

$$\hat{P}(\theta_t, \theta_r) = \frac{1}{(\mathbf{a}(\theta_t) \otimes \mathbf{b}(\theta_r))^H \mathbf{R}_{YY}^{-1}(\mathbf{a}(\theta_t) \otimes \mathbf{b}(\theta_r))}, \quad (6)$$

where $\mathbf{R}_{YY} = \frac{1}{Q}\mathbf{Y}\mathbf{Y}^H$.

In case of perfect array calibration, $\mathbf{a}(\theta_t)$ and $\mathbf{b}(\theta_r)$ are known functions of θ_t, θ_r and the targets are localized by searching for the peaks in the 2-D spectrum $\hat{P}(\theta_t, \theta_r)$, which is computed for every pair of angles of interest. As noticed in [4], this 2-D imaging method fails to work for closely located targets, since a single lobe may then occur in the spectrum $\hat{P}(\theta_t, \theta_r)$ for such targets. Moreover, (6) relies on the estimation of the sample covariance matrix of the observed signals, which in turn requires the signals to be observed over a sufficiently long time interval. Finally, this approach requires a two-dimensional angular scanning which may become highly time consuming for a dense angular grid.

In the following section, we propose a deterministic alternative to the 2D-Capon method (6) for detection and localization of the K targets, which has none of the aforementioned drawbacks. By recognizing that (5) is a PARAFAC model, it follows that exploitation of the algebraic structure of $\mathbf{Y}$ is sufficient for unique estimation of $\mathbf{A}(\theta_t)$, $\mathbf{B}(\theta_r)$ and $\mathbf{C}$, up to trivial indeterminacies only (arbitrary scaling and permutation of the columns).

3. REFORMULATION IN TERMS OF PARAFAC ANALYSIS

Let us first define the Parallel Factor decomposition of a third-order tensor.

Definition 1. (PARAFAC in tensor format)

A PARAFAC decomposition [5] of a tensor $\mathcal{Y} \in \mathbb{C}^{I \times J \times K}$ is a decomposition of the type $\mathcal{Y} = \sum_{r=1}^R \mathbf{a}_r \circ \mathbf{b}_r \circ \mathbf{c}_r$, where $\mathbf{a}_r, \mathbf{b}_r, \mathbf{c}_r$ are the rth columns of the so-called "loading matrices" $\mathbf{A} \in \mathbb{C}^{I \times R}$, $\mathbf{B} \in \mathbb{C}^{J \times R}$ and $\mathbf{C} \in \mathbb{C}^{K \times R}$, respectively, and $\circ$ is the outer product, i.e., $(\mathbf{a}_r \circ \mathbf{b}_r \circ \mathbf{c}_r)_{ijk} = a_{ir}b_{jr}c_{kr}$, for all values of the indices i, j and k.

Definition 2. (PARAFAC in matrix format)

Let $\mathbf{Y}^{(1)} \in \mathbb{C}^{IJ \times K}$, $\mathbf{Y}^{(2)} \in \mathbb{C}^{KI \times J}$ and $\mathbf{Y}^{(3)} \in \mathbb{C}^{JK \times I}$ be the three standard matrix representations of $\mathcal{Y} \in \mathbb{C}^{I \times J \times K}$, such that $[\mathbf{Y}^{(1)}]_{(i-1)J+j,k} = y_{ijk}$, $[\mathbf{Y}^{(2)}]_{(k-1)I+i,j} = y_{ijk}$ and $[\mathbf{Y}^{(3)}]_{(j-1)K+k,i} = y_{ijk}$. The PARAFAC decomposition of $\mathcal{Y}$ can then be written under the three following equivalent matrix forms: $\mathbf{Y}^{(1)} = (\mathbf{A} \odot \mathbf{B})\mathbf{C}^T$, $\mathbf{Y}^{(2)} = (\mathbf{C} \odot \mathbf{A})\mathbf{B}^T$ and $\mathbf{Y}^{(3)} = (\mathbf{B} \odot \mathbf{C})\mathbf{A}^T$.

Let us now build the observed tensor $\mathcal{Y}$ and the noise tensor $\mathcal{Z}$ of size $M_r \times M_t \times Q$, obtained by stacking the Q matrices $\mathbf{Y}_q$ and $\mathbf{Z}_q$ defined in (3) along the third dimension, respectively. From definition 2, it is clear that (5) corresponds to the PARAFAC decomposition, written in matrix format, of the noisy observed tensor $\mathcal{Y}$. Once this link established, it follows that the problem of detection and localization of multiple targets can be considered from a deterministic perspective, by capitalizing on the strong algebraic structure of the observed data rather than their statistics.

4. IDENTIFIABILITY, DETECTION AND LOCALIZATION

4.1. Identifiability

The PARAFAC decomposition of $\mathcal{Y} \in \mathbb{C}^{M_t \times M_r \times Q}$ is said to be *essentially unique* if any matrix triplet $\tilde{\mathbf{A}}(\theta_t) \in \mathbb{C}^{M_t \times K}$, $\tilde{\mathbf{B}}(\theta_r) \in \mathbb{C}^{M_r \times K}$ and $\tilde{\mathbf{C}} \in \mathbb{C}^{Q \times K}$ that fits the model is related to $\mathbf{A}(\theta_t)$, $\mathbf{B}(\theta_r)$ and $\mathbf{C}$ via $\mathbf{A}(\theta_t) = \tilde{\mathbf{A}}(\theta_t)\mathbf{\Pi}\mathbf{\Lambda}_1$, $\mathbf{B}(\theta_t) = \tilde{\mathbf{B}}(\theta_t)\mathbf{\Pi}\mathbf{\Lambda}_2$ and $\mathbf{C} = \tilde{\mathbf{C}}\mathbf{\Pi}\mathbf{\Lambda}_3$ with $\mathbf{\Lambda}_1$, $\mathbf{\Lambda}_2$, $\mathbf{\Lambda}_3$ arbitrary diagonal matrices satisfying $\mathbf{\Lambda}_1\mathbf{\Lambda}_2\mathbf{\Lambda}_3 = \mathbf{I}_K$ and $\mathbf{\Pi}$ a permutation matrix.

If no specific structure is assumed on the loading matrices, identifiability conditions that guarantee essential uniqueness can be found in [6, 7]. If $\mathbf{A}(\theta_t)$ and $\mathbf{B}(\theta_r)$ have a Vandermonde structure and $\mathbf{C}$ has no specific structure, a first sufficient condition for essential uniqueness has been derived in [8]. A more relaxed condition was then proven in [9]. The latter is given by the following theorem.

Theorem 1: Assume that the generators of the Vandermonde matrices $\mathbf{A}(\theta_t)$ and $\mathbf{B}(\theta_r)$ are drawn from a continuous distribution and that $\mathbf{C}$ is full column rank. If

$$\max(M_t, M_r) \geq 3 \text{ and } K \leq M_t M_r - \min(M_t, M_r), \quad (7)$$

then the PARAFAC decomposition of $\mathcal{Y} \in \mathbb{C}^{M_t \times M_r \times Q}$ is almost-surely essentially unique.

The first assumption of this theorem implies that $\mathbf{A}(\theta_t) \odot \mathbf{B}(\theta_r)$ is almost-surely full rank [9], which is generically satisfied in practice. The second assumption is also generically satisfied, provided that $Q \geq K$, since our target model is a classical Swerling II with RCS fluctuations varying independently from pulse to pulse.

4.2. Detection of multiple targets

The maximum number of targets that can be identified is given by (7). Provided that Theorem 1 is satisfied, $(\mathbf{A}(\theta_t) \odot \mathbf{B}(\theta_r))\mathbf{C}^T$ is generically rank K. It follows that the number of targets K can be estimated as the number of significant singular values of $\mathbf{Y}$, i.e., the singular values associated to the signal subspace.

4.3. Localization of multiple targets

Suppose that the number of targets is known or has been estimated and satisfies uniqueness of the PARAFAC decomposition of $\mathcal{Y}$. A PARAFAC model with K components is first optimally fitted on the observed tensor $\mathcal{Y}$. This can be done by various optimization algorithms [10] or a simultaneous-diagonalization based algorithm [7], that we will use in practice. These algorithms, in their original form, do not impose a specific structure on the estimates $\hat{\mathbf{A}}(\theta_t)$, $\hat{\mathbf{B}}(\theta_r)$ or $\hat{\mathbf{C}}$. In practice, we recover the manifold structure of $\hat{\mathbf{A}}(\theta_t)$ and $\hat{\mathbf{B}}(\theta_r)$ a posteriori, i.e., after convergence.

For instance, in the ULA case, the Vandermonde structure is recovered as follows. We first build the $(M_t - 1) \times 1$ vector $\mathbf{d}(\theta_{t_i}) = [\hat{\mathbf{a}}(\theta_{t_i})]_{2:M_t} ./[\hat{\mathbf{a}}(\theta_{t_i})]_{1:M_t - 1}$, where $./$ is the element-wise division and $\hat{\mathbf{a}}(\theta_{t_i})$ is the ith column of $\hat{\mathbf{A}}(\theta_t)$. The $M_t - 1$ points of $\mathbf{d}(\theta_{t_i})$ are averaged to get and estimate of $e^{-j\frac{2\pi}{\lambda}d_t \sin(\theta_{t_i})}$, where d_t is the inter-element spacing at the transmitter and λ the carrier wavelength. The same procedure is applied to every column of $\hat{\mathbf{A}}(\theta_t)$, to build the set $\{\hat{\theta}_{t_k}\}_{k=1}^K$. We proceed similarly to estimate the angles $\{\hat{\theta}_{r_k}\}_{k=1}^K$ from $\hat{\mathbf{B}}(\theta_r)$. Note that the uniqueness property of PARAFAC implies that the transmit and receive angles relative to the same target are automatically paired.

5. EXPERIMENTAL RESULTS

We generate the observed matrices $\mathbf{X}_q$, $q = 1, \ldots, Q$, in (1) as follows. The mth transmitted waveform, i.e., the mth row of $\mathbf{S}$, is generated by $[\mathbf{S}]_{m,:} = \frac{1+j}{\sqrt{2}}[\mathbf{H}_N]_{m,:}$, where $\mathbf{H}_N$ is the $N \times N$ Hadamard matrix, and N is fixed to 256. We consider ULA transmit and receive arrays with $\lambda/2$ inter-element spacing for both arrays. The carrier frequency is fixed to 1 GHz. Following the Swerling Case II target model, we assume that the reflection coefficient β_k of the kth target obeys the complex Gaussian distribution with zero mean and unknown variance $\sigma_{\beta_k}^2$. Let us denote by $\mathcal{X} \in \mathbb{C}^{M_r \times N \times Q}$ and $\mathcal{W} \in \mathbb{C}^{M_t \times N \times Q}$ the tensors obtained by stacking the matrices $\{\mathbf{X}_q\}_{q=1}^Q$ and $\{\mathbf{W}_q\}_{q=1}^Q$ in (1), respectively, along the third-dimension. We assume that the elements of the noise and interference tensor $\mathcal{W}$ obey a complex Gaussian distribution with zero mean and unknown variance. The Signal to Noise Ratio (SNR) at the input of the receiver is defined by $\text{SNR} = 10\log_{10}(\frac{\|\mathcal{X}^{(s)}\|_F^2}{\|\mathcal{W}\|_F^2})$ [dB], where $\mathcal{X}^{(s)}$ is the noise-free part of $\mathcal{X}$ and $\|\cdot\|_F$ is the Frobenius norm.

In a first experiment (Fig. 1), we compare the performance of our PARAFAC-based method to the 2-D Capon beamforming method (6) proposed in [4], for the two cases $M_t = M_r \in \{4, 6\}$, with SNR = 8 dB and $Q = 500$ pulses. We consider $K = 9$ targets, with transmit and receive angles (in degrees) $\{\theta_{t_k}\}_{k=1}^K = \{-60, -40, -30, 0, 10, 20, 30, 50, 60\}$ and $\{\theta_{r_k}\}_{k=1}^K = \{-20, 70, 40, 0, -60, -50, -40, -10, 50\}$, respectively. The set $\{\sigma_{\beta_k}^2\}_{k=1}^K$ holds linearly spaced values from 0.3 to 0.7. Figs. (1(a)) and (1(c)) represent the "contour" plot of $\hat{P}(\theta_t, \theta_r)$ defined in (6), computed for every pair of transmit and receive angles ranging from $-90°$ to $90°$ with an angular step-size of $0.5°$. With 4 receive and 4 transmit antennas, 2-D Capon does not allow accurate localization of all targets. For instance, the three closely spaced targets localized at $\{\theta_{t_k}\}_{k=5}^7 = \{10, 20, 30\}$, $\{\theta_{r_k}\}_{k=5}^7 = \{-60, -50, -40\}$ can not be distinguished. On the contrary, PARAFAC allows relatively accurate localization of all targets. When the number of antennas increases from $M_t = M_r = 4$ to $M_t = M_r = 6$, the performance of 2-D Capon improves but PARAFAC remains more accurate. Another major advantage
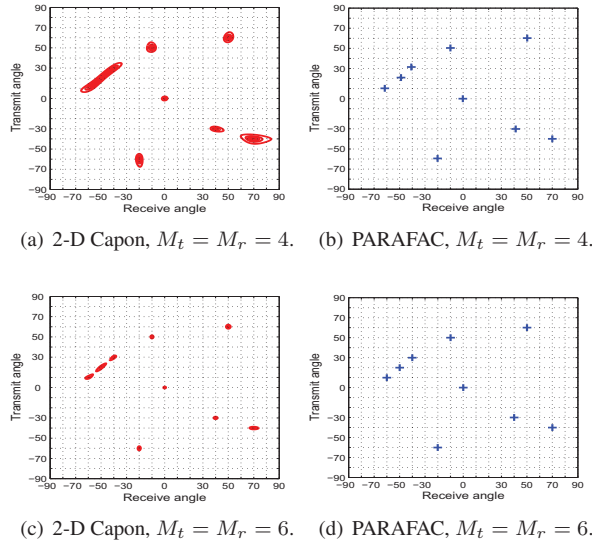
(a) 2-D Capon, $M_t = M_r = 4$. (b) PARAFAC, $M_t = M_r = 4$.

(c) 2-D Capon, $M_t = M_r = 6$. (d) PARAFAC, $M_t = M_r = 6$.

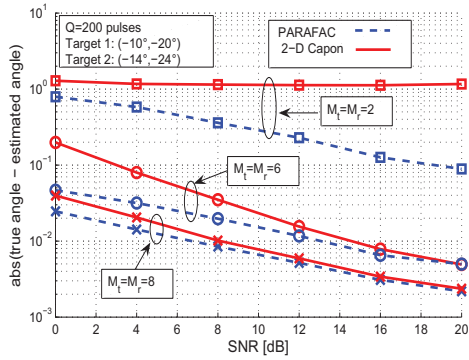**Fig. 1**. SNR=8dB. $Q = 500$ pulses. $K = 9$ targets.

Fig. 2. Impact of the number of antennas on the performance of PARAFAC and 2-D Capon.

of PARAFAC over 2-D Capon is its low complexity. For instance, in this experiment, PARAFAC converged after 0.25 sec while 2-D Capon required 28 sec for computing (6) for all pairs of angles.

In a second experiment (Fig. 2), we compare both methods via Monte-Carlo simulations. The performance criterion is the absolute value of the difference between the true angle and estimated angle, averaged over transmit and receive angles and over all targets. We simulate the presence of two targets, characterized by $(\theta_{t_1}, \theta_{r_1}) = (-10°, -20°)$, $\sigma_{\beta_1}^2 = 0.35$ and $(\theta_{t_2}, \theta_{r_2}) = (-14°, -24°)$, $\sigma_\beta^2 = 0.4$, respectively. The number of pulses is $Q = 200$. For each SNR value, we have conducted 100 Monte-Carlo runs. For the comparison between methods to be fair, the angular resolution for 2-D Capon is fixed to $0.001°$. Since scanning all angles between $-90°$ and $90°$ with such a small angular step-size takes too

long, we proceed as follows. The first round of scanning is done with a step-size of $1°$, to get a first localization of the two highest peaks of $\hat{P}(\theta_t, \theta_r)$. Then the estimation is refined individually for each target around those peaks in several rounds, to reach the final resolution of $0.001°$. Performance is assessed in three cases: $M_t = M_r \in \{2, 6, 8\}$. We observe that PARAFAC outperforms 2-D Capon in all cases. As expected, the performance of both techniques improves when the number of antennas increases. Note that 2-D Capon fails with $M_t = M_r = 2$, because the targets are too close to each other for the two lobes to be clearly distinguishable in the Capon spectrum.

6. CONCLUSION AND FUTURE WORK

We have shown that the detection and DOA-DOD estimation of multiple targets in a bistatic MIMO radar system can be accomplished by the PARAFAC decomposition of the observed data tensor. Unlike conventional radar imaging approaches, the proposed method is deterministic and fully capitalizes on the algebraic structure of the data, rather than on their statistics. Simulation results illustrate the potential of our technique, which outperforms the 2-D Capon method proposed in [4], at a lower complexity. Future work includes the derivation of adaptive PARAFAC algorithms for DOA-DOD tracking.

REFERENCES

[1] J. Li and P. Stoica, "MIMO Radar with Colocated Antennas," *IEEE Signal Processing Magazine*, pp. 106–114, Sep. 2007.

[2] A. Haimovich, R. S. Blum, and L. J. Cimini Jr., "MIMO Radar with Widely Separated Antennas," *IEEE Signal Processing Magazine*, pp. 116–129, Jan. 2008.

[3] L. Xu, J. Li, and P. Stoica, "Radar imaging via adaptive MIMO techniques," in *Proc. 14th European Signal Proc. Conf.*, Florence, Italy, Sept. 2006.

[4] H. Yan, J. Li, and G. Liao, "Multitarget Identification and Localization Using Bistatic MIMO Radar Systems," *EURASIP Journal on Advances in Sig. Proc.*, vol. 2008, no. ID 283483, 2008.

[5] R. A. Harshman, "Foundations of the PARAFAC procedure: Model and Conditions for an 'explanatory' Multi-mode Factor Analysis," *UCLA Working Papers in Phonetics*, vol. 16, pp. 1–84, 1970.

[6] N. D. Sidiropoulos and R. Bro, "On the Uniqueness of Multilinear Decomposition of N-way Arrays," *Journal of Chemometrics*, vol. 14, pp. 229–239, 2000.

[7] L. De Lathauwer, "A Link between the Canonical Decomposition in Multilinear Algebra and Simultaneous Matrix Diagonalization," *SIAM J. Matrix Anal. Appl.*, vol. 28, no. 3, pp. 642–666, 2006.

[8] N. D. Sidiropoulos and X. Liu, "Identifiability Results for Blind Beamforming in Incoherent Multipath with Small Delay Spread," *IEEE Trans. Signal Proc.*, vol. 49, no. 1, pp. 228–236, 2001.

[9] T. Jiang, N. D. Sidiropoulos, and J. M.F. ten Berge, "Almost Sure Identifiability of Multidimensional Harmonic Retrieval," *IEEE Trans. Signal Proc.*, vol. 49, no. 9, pp. 1849–1859, 2001.

[10] G. Tomasi and R. Bro, "A Comparison of Algorithms for Fitting the PARAFAC Model," *Comp. Stat. Data Anal.*, vol. 50, pp. 1700–1734, 2006.